MULTIPLE EVENT ANALYSIS OF 1979 IMPERIAL VALLEY, CALIFORNIA EARTHQUAKE USING DISTINCT PHASES IN NEAR-FIELD ACCELEROGRAMS

Yozo FUJINO (I)
Takashi YOKOTA (II)
Yoshihiro HAMAZAKI (III)
Ryosuke INOUE (IV)
Presenting Author: Y. FUJINO

SUMMARY

Distinct phases in the horizontal accelerograms of the 1979 Imperial Valley earthquake are identified by two methods; one is a visual inspection method and the other a quantitative method. Next, the location of the source corresponding to the identified distinct phases is determined using the S-wave travel-time curve. It is found by the two methods that the earthquake is a multiple event with three smaller events in the period of less than 1 to 2 second and that the main energy of this period range is released from a localized area about 10 to 13 km to north from the epicenter. The results are compared with the spatial dislocation model of this earthquake obtained by Hartzell and Helmberger(1).

INTRODUCTION

In view of the engineering and seismological importance of near-field strong motion records, the U.S. Geological Survey and some other organizations installed many strong-motion accelerographs near the Imperial fault, California in 1975 and received a rewarding result from the 1979 Imperial Valley earthquake(2).

The objective of this paper is to identify the multiple rupture process of the 1979 Imperial Valley earthquake using the accelerograms recorded in the Imperial Valley, California and the Northern Baja, Mexico strong-motion network and to study the effect of the source characteristics on the near-field acceleration motions.

Recent seismological studies (for example Refs. 3-6) indicate that most large earthquakes are complex multiple events in the periods of ten to several tens second. Trifunac and Brune (7) interpreted that the main shock of the 1940 Imperial Valley earthquake was a multiple event even in the periods of less than 1 second and discussed the importance of the multipleness of the rupture process from the engineering viewpoint. Their interpretation is based on the visual looking of the single three-component accelerogram recorded at El Centro during that earthquake. Since nearly 30 near-field accelerograms are available in the 1979 event, more reliable analysis of multiple event in this period range can be expected even though the same method is employed.

(I) Assoc. Professor of Civil Eng., Univ. of Tokyo, Tokyo, Japan 113
(II) Seismologist of Meteorological Res. Inst., Tsukuba, Ibaraki, Japan
(III) Res. Engineer, Kobe Steel Co., Ltd., Kobe, Japan
(IV) Res. Assoc. of Construction Eng., Univ. of Ibaraki, Ibaraki, Japan

Methods of multiple event analysis used in the seismology can be divided into two; the distinct phase method(5,6,7,10) and the waveform matching method(3,4). The distinct phase method is to identify distinct phases in seismograms and to determine the location of the sources which generate such distinct phases, revealing the multipleness of an earthquake. On the other hand, the waveform matching method is to construct a multiple dislocation model such that the synthetic ground motion(s) computed by the model agrees well with the recorded seismogram(s). The distinct phase method is employed in this study.

The October 15, 1979 Imperial Valley earthquake occurred at the well-defined Imperial fault. In Fig. 1 the location of the accelerographs triggered by the 1979 earthquake as well as the location of the causative fault is shown. One can see that the accelerographs are installed in various azimuthes and distances from the fault. It should be noted that more than ten of the accelerograms had absolute trigger timing with millisecond accuracy.

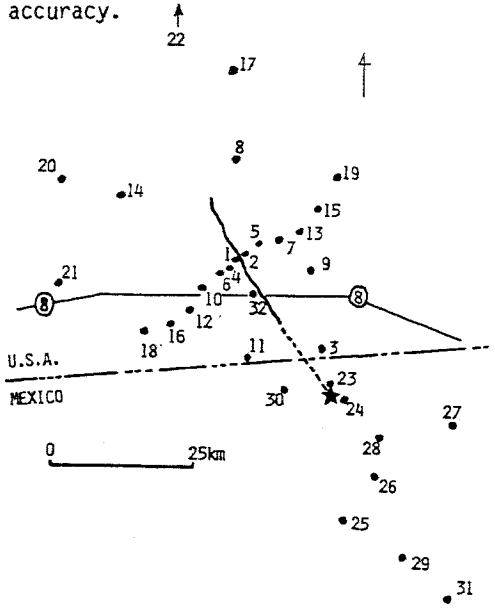

1	El Centro Array 7	17	Calipatria
2*	El Centro Array 6	18*	El Centro Array 13
3*	Bonds Corner	19*	El Centro Array 1
4*	El Centro Array 8	20	Superstiton Mt.
5*	El Centro Array 5	21	Plaster City
6	El Centro Diff. Array	22	Coachella
7*	El Centro Array 4	23	Aeropuetro(Mexico)
8*	Brawley Airport	24	Agrarias(")
9	Holtville	25	Cerro Prieto(")
10	El Centro Array 10	26	Chihuahua(")
11*	Calexico	27	Compuertas(")
12*	El Centro Array 11	28	Cucapah(")
13	El Centro Array 3	29	Delta(")
14	Parachute	30	Mexicali SAHOP(")
15*	El Centro Array 2	31	Victoria(")
16*	El Centro Array 12	32	Meloland

*; absolute trigger time available

Fig. 1 Imperial valley strong-motion network and causative Imperial fault

The focal depth is determined using the first S-wave arrival in accelerograms and the S-wave travel-time calculated from the crustal model (Fig. 2) of this region proposed by Fuis et al.(11). It is found that the focal depth of 7 km is the most appropriate value and is used in the multiple event analysis which follows.

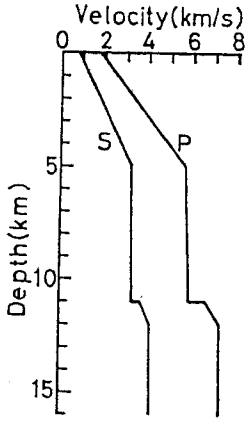

Fig. 2 Crustal model(11) : S- and P- wave velocity

ANALYSIS

Identification of Distinct Phases in Accelerograms

I) Visual Inspection Method

The distinct phase in seismograms or accelerograms

can be defined as the phase when the amplitude and(or) the phase of the motion change abruptly as compared with the preceding motion. In this study the acceleration motions corrected from the original accelerograms under a standard routine(9) are resolved into various frequency range in order to facilitate identification of distinct phases. Fig. 3 shows examples of accelerations, filtered accelerations and identified distinct phases denoted by arrows. We could observe distinct phases rather clearly in the records of the Mexican side. This is probably due to the direction of the fault rupture.

Identifying distinct phases is made on the basis of authors' subjective judgment. To establish an objective criterion of the procedure is highly desired although this seems to be very difficult from our experience. An attempt of a quantitative approach follows.

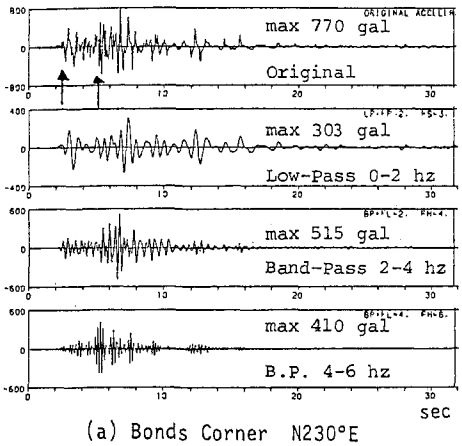

(a) Bonds Corner N230°E

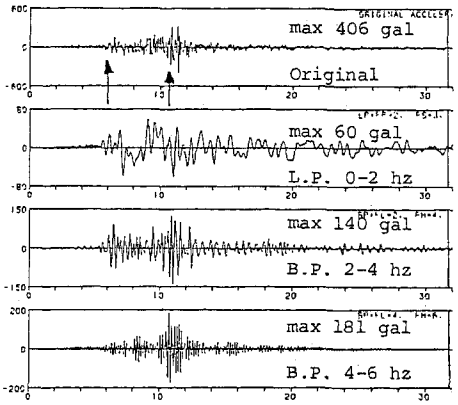

(b) El Centro Array No.2 N230°E

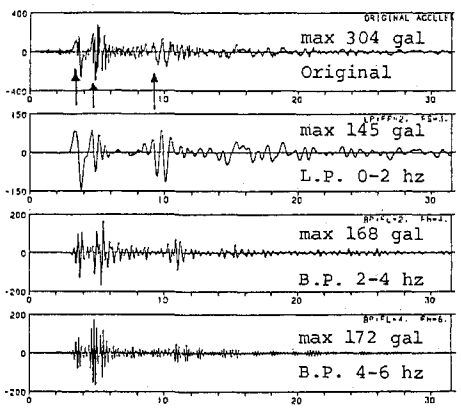

(c) Cucapah(Mexico) N85°E

Fig. 3 Examples of (filtered) acceleration and distinct phases identified by visual inspection

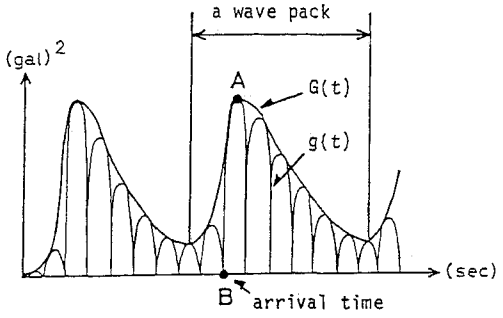

Fig. 4 Definition of arrival time of distinct phase by quantitative method

II) Quantitative Method

The near-field ground motion due to multiple event would have multiple peaks in its envelope as shown in Fig. 4. Each wave pack may be considered to correspond to individual event. Let g(t) be defined as $x^2(t) + y^2(t)$

where x(t) and y(t) are the two horizontal acceleration components of an accelerogram and G(t) be the envelope of g(t). In Fig. 4 , the amplitude of G(t) takes the local maximum at the point A. The point B where g(t) takes the local minimum just before the point A, may correspond to the arrival time of the large seismic wave energy. In this quantitative approach the point B is defined as the arrival of the distinct phase generated by an event.

The original acceleration motions are resolved into three filtered motions with 0-2Hz, 2-4Hz and 4-6Hz width, respectively. In each filtered motion, the arrival time of the distinct phases (point B) is determined according to the aforementioned criterion. The following rank is assigned to each identified distinct phase depending on the ratio r of the local maximum amplitude of G(t) to the absolute maximum of G(t); the rank is 3 for r = 0.4-0.6, 4 for r = 0.6-0.8, and 5 for r = 0.8-1.0, respectively. Fig. 5 shows an example of g(t) and G(t). In this criterion, it is found that the S-wave arrival coming from the epicenter is not always identified as the distinct phase with a high rank even though it is clearly identified as the distinct phase by visual inspection. This is because the S-wave arrival from the epicenter is not necessarily large in amplitude. Obviously there are some minor drawbacks in this quantitative criterion and further improvement is certainly needed.

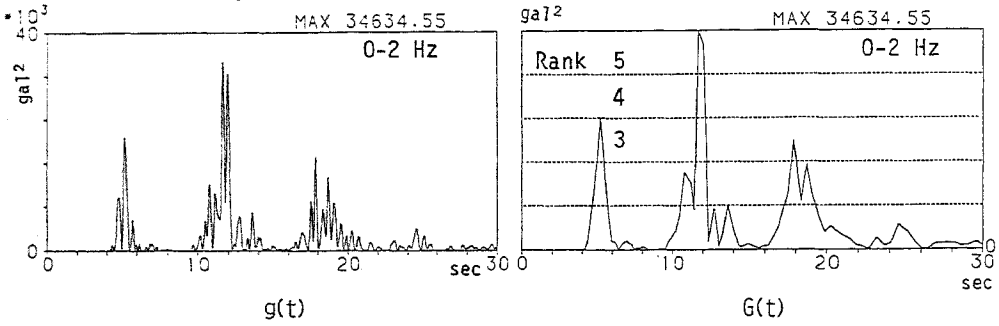

Fig. 5 An example of squared wave g(t) and its envelope G(t) and rank of distinct phase

Determination of Location of Source Corresponding to Distinct Phase

Location of the source which corresponds to the distinct phases in each accelerograms is determined as follows. The causative fault of 35 km length is divided into 23 small fault segments. The absolute arrival time T_i of the seismic wave due to the i-th fault segment in the station is given by

$$T_i = t_0 + \frac{L_i}{V_r} + t_i \qquad (1)$$

where t_0 = origin time, L_i = distance from the epicenter to the i-th fault segment along the fault, V_r = rupture velocity, t_i = S-wave travel-time of seismic waves from the i-th segment to the station.

In order to utilize the horizontal accelerograms having no absolute trigger timing, the trigger times for such accelerograms are estimated using

the S-wave travel curves. In this procedure it is assumed that the first S-wave arrival in the accelerograms came from the epicenter. Table 1 presents the trigger time minus the origin time (T-O time) at the stations. Note that trigger time at the station 7 is corrected because the available absolute trigger time is found questionable. The trigger times at the other stations with timing available are judged to be correct.

Table 1 Trigger time minus origin time (T-O time) estimated from S-wave travel-time curve

Station	T-O(sec)	Station	T-O(sec)	Station	T-O(sec)
1	6.5	10	6.2	19*	7.74
2*	6.9	11*	4.37	21	14.8
3*	2.61	12*	5.98	24	4.2
4*	6.12	13	7.0	25	5.3
5*	6.89	14	10.0	26	4.5
6	6.0	15*	6.68	27	9.8
7#	6.8	16*	6.98	28	3.8
8*	9.04	17	14.0	29	6.5
9	5.0	18*	7.95	31	10.1

* :Trigger time available
\# :Trigger time available but corrected

Since the arrival times of distinct phases in horizontal accelerograms are determined in the previous section, the distance L_i, i.e. location of the source corresponding to the identified distinct phase can be calculated by Eq. 1 under an assumed value of rupture velocity V_r.

RESULTS AND DISCUSSION

According to the procedure explained above, the location of the sources corresponding to the distinct phases identified by the visual inspection is calculated and the results for the rupture velocity V_r = 2.5 km/s (1) are presented in Fig. 6. The numbers in Fig. 6 denote the stations whose locations are shown in Fig. 1. Note that the results in Fig. 6 were found not sensitive for V_r = 2.3-2.5 km/s

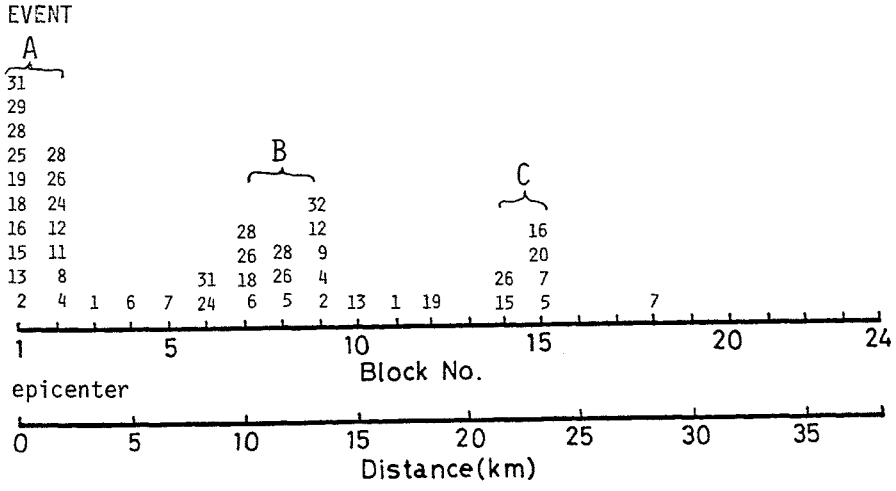

Fig. 6 Distribution of distinct phases on fault (identified by visual inspection)

Fig. 6 shows that the 1979 earthquake roughly consists of three events, A, B and C. Many stations identified the event A. This is because the first S-wave arrival possibly from the epicenter can be, in general, clearly observed. Therefore it cannot be concluded that the large seismic energy is released at the event A. A number of the stations identified the event B locating at the distance 10-13 km from the epicenter. Distinct phase in the middle part of the strong motions is generally not observed clearly unless its amplitude changes appreciably in comparison with that of the preceding motion. Taking this into account, the event B would be the largest event releasing the bulk of seismic energy in the period range of less than 1 to 2 second.

Next, the results by the quantitative method are presented in Fig. 7, where the ordinate is the total score and the abscissa is the distance from the epicenter along the fault. Note that the score is the sum of the ranks of distinct phases in the three filtered motions of each accelerograms. The rupture velocity is assumed to be 2.3 km/s. The total score in Fig. 7 is computed using only the ranks 3, 4 and 5. The score with shade is obtained

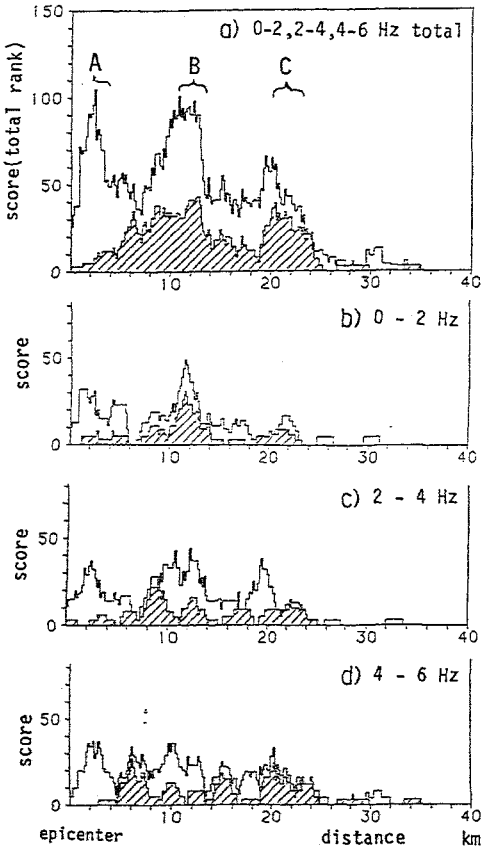

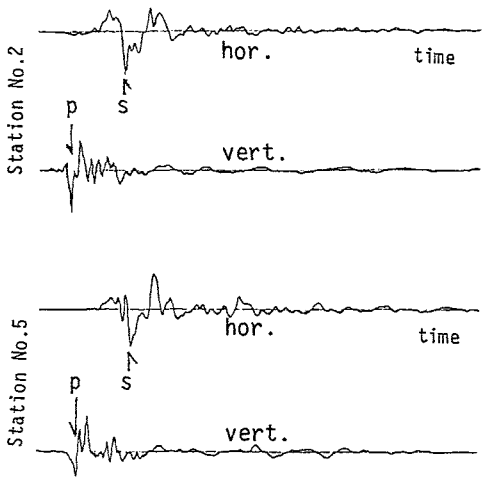

Fig. 8 Corresponding S- and P- distinct phases (0-2 Hz filtered accelerations)

Table 2 Rupture velocity and location of event calculated from S- and P- distinct phases (see Fig. 8)

Station	S-P(sec)	Position of Event (km)	Vr(km/sec)
2	3.49	11.8	2.21
5	3.39	12.9	2.29
19	5.08	11.6	2.35

Fig. 7 Distribution of score of distinct phases by quantitative method

from the accelerograms with the known absolute timing while the score without shade is from all the accelerograms.

Fig. 7 b), c) and d) show the distribution of the total score for the three frequency ranges. In the longer period ground motion (0-2 Hz) the clusters of score, especially at the location at 12 km distance from the epicenter can be observed whereas in shorter period motion (4-6 Hz) total score is rather uniformly distributed. This may indicate that the spatial distribution of generation of seismic waves on a fault is dependent on the frequency.

The rupture velocity can be principally estimated from the S-P time of the distinct phase in horizontal and vertical accelerograms. Fig. 8 shows examples of 0-2 Hz band-pass filtered acceleration motions where distinct phases of S and P waves can be identified and are probably from the same event. Table 2 presents the rupture velocity and the location of the event calculated from S-P time of these accelerograms. This result also supports that the rupture velocity is approximately 2.3 km/s and that one event is located at approximately 12 km distance from the epicenter.

According to the visual inspection as well as the quantitative criterion, it is found that this earthquake is a multiple event sequence with 3 events. The event A is located near the epicenter and B is approximately 12 km distant from the epicenter while the event C is located at 20 km distance or so as shown in Figs. 6 and 7. The size of the three events is of engineering concern. Utilizing the work by Kanamori and Jennings (13) and by Luco (14), the local magnitudes M_L of these three events are calculated from the accelerograms; average M_L of event A = 5.8, similarly M_L of event B = 6.3, and M_L of event C = 6.1. M_L of this earthquake calculated from the same accelerograms by Luco(14) is 6.3 (average) although M_L reported by USGS is 6.6. Conclusively, the event B is the largest event among the three and released the most of the seismic wave energy of the period less than 1-2 second.

Hartzell and Helmberger(1) obtained, by the waveform matching method, a two-dimensional fault dislocation model to explain twelve three-component strong-motion displacement records of this earthquake. It should be noted that major period consisting of the displacement motion is around 5 second which is longer than the period range considered in this analysis. Their preferred model has two localized areas of larger dislocations as shown in Fig. 9; one just north

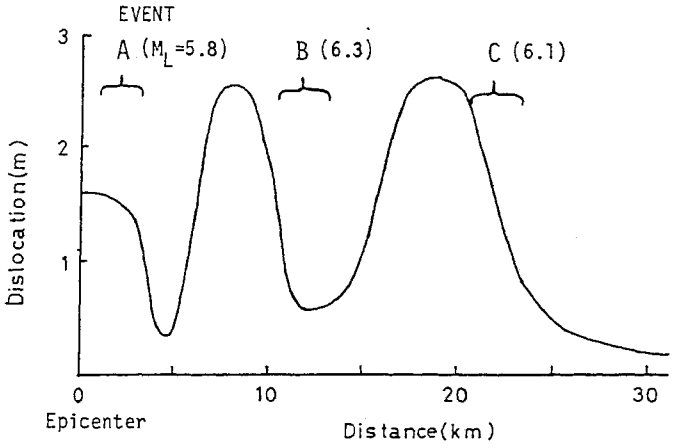

Fig. 9 Dislocation distribution by Hartzell and Helmberger and location of events A,B and C determined in this study

of the border near Bonds Corner (approximately 8 km from the epicenter), a second under Interstate 8 at Meloland Overpass (approximately 18 km from the epicenter). Comparing the results in Figs. 6 and 7a) with that in Fig. 9, one can find the events B and C obtained in this study are not completely coincident in location to the localized areas of larger dislocation calculated by Hartzell and Helmberger and are located at the ending part of the localized areas having large dislocation. This implies that large dislocation does not necessarily generate a large amount of seismic waves of the period less than 1-2 second. If the portion of the fault with small dislocation may be called 'barrier', apparently, such short-period seismic waves are mostly generated when the fault rupture approaches the barriers.

CONCLUDING REMARKS

An analysis of the multiple rupture process of the 1979 Imperial Valley earthquake is made by identifying distinct phases in the near-field horizontal accelerograms. In the identification, visual inspection method and quantitative method are employed. It is found by the two methods that this earthquake is a multiple event with three smaller events A, B and C in the period range of less than 1 to 2 second, indicating that the short period seismic waves were mainly released from the localized areas of the fault.

The event B at approximately 12 km distance from the epicenter has the local magnitude M_L of 6.3 which is almost equal to M_L of this earthquake and is found to be the largest event among the three. The results are compared with the spatial dislocation model obtained by Hartzell and Helmberger(1) and it is found that location of the events A, B and C is not completely coincident to the localized areas having large dislocation. The comparison implies that large amount of short-period seismic waves are released when the fault rupture approaches the barriers where the dislocation is small.

References

1) Hartzell, S. and D. V. Helmberger, BSSA, Vol. 72, 2, 1982.
2) Matthiesen R. B. and R. L. Porcella, CIRC 818-C, USGS, 1981.
3) Kanamori, H. and G. S. Stewart, J. Geophys. Res. 83, 1978.
4) Kikuchi, M. and H. Kanamori, BSSA., Vol. 72, 2, 1982.
5) Fukao, Y. and M. Furumoto, Phys. Earth Planet. Inter., 10, 1975.
6) Seno, T. et al., Phys. Earth Planet. Inter., 23, 1980.
7) Trifunac, M. D. and J. N. Brune, BSSA, Vol. 60, 1, 1970.
8) Archuleta, R. J., BSSA, Vol. 72, 5, 1982.
9) Brady, A. G. et al., USGS. Open-File Report 80-703, 1980.
10) Nagamune, J. Seism. Soc. Japan, Vol. 22, 2, 1969 (in Japanese).
11) Fuis, G. S. et al., USGS Profess. Paper 1254, 1982.
12) Saito, M., Geophysical Exploration, Vol. 31, 4, 1978 (in Japanese).
13) Kanamori, H. and P. C. Jennings, BSSA, Vol. 61, 2, 1978.
14) Luco, J. E., BSSA, Vol. 72, 3, 1982.